Journal of Materials Chemistry C

Accepted Manuscript

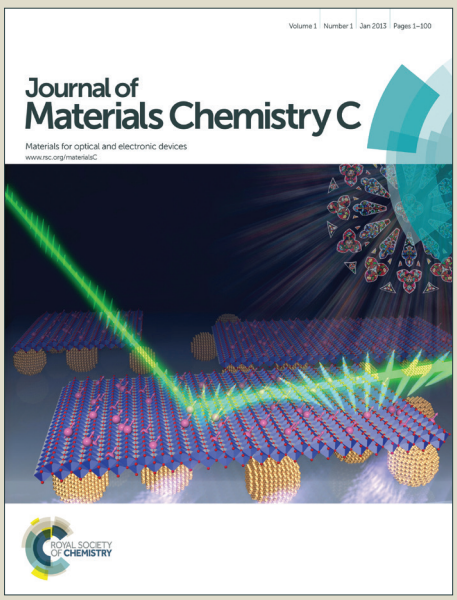

ROYAL SOCIETY OF CHEMISTRY

www.rsc.org/materialsC

Efficient Infrared Photodetector based on Three-Dimensional Self-Assembly PbSe Superlattices

Lei Qian*, Yixing Yang, Changfeng Han, Yuanyuan Cheng and Ling Chen

Key Lab for Special Functional Materials of Ministry of Education, Henan University, Kaifeng 475004 P. R. China

Ting Zhang* and Wei Xue

School of Optoelectonics, Beijing Institute of Technology, Beijing, China, 100081

Debasis Bera and Paul H. Holloway*

Department of Materials Science and Engineering, University of Florida, Gainesville, FL 32611-6400

Abstract:

We report an efficient infrared (IR) photodetector using three-dimensional self-assembly Lead Selenide (PbSe) superlattices as an absorber. These self-assembly superlattices were synthesized by using a hot solution method where the size of superlattice could be varied by controlling the reaction time and concentration of surfactants including TOP, TOPO and oleic acid. It was found that the interactions between surfactants were the major driven force for this self-organization behavior, while surface charges would also affect the self-assembly process of superlattices. Infrared photodetector with device structure ITO/PEDOT:PSS/PbSe superlattices/ZnO nanoparticles/Al showed high detectivity of 4×10^{10} Jones at 3V bias under 830 nm infrared irradiation.

*Corresponding Author Lei Qian qian_lei@126.com; Ting Zhang zhangting@bit.edu.cn ; Paul H Holloway pholl@mse.ufl.edu

Lead chalcogenide colloidal nanoparticles have attracted growing interest due to its potential applications on Infrared (IR) optoelectronics such as IR light emitting diodes (LED), photodetectors and solar cells [1-5]. However, the optoelectronic properties of Lead chalcogenide nanoparticles are size-dependent and not fully match the requirements for high efficiency optoelectronic devices [6-11]. For example, emission wavelength of colloidal nanoparticles can be tuned by varying their sizes due to quantum confinement effect, which requires the particle size should smaller than its Bohr radius. On the other hand, the thickness of functional layers in optoelectronic devices are usually in the range of 50-500 nm, which reduced carriers transport ability or excitons diffusion length because charge carriers or excitons could pass through the functional layer by hopping multiple times between neighboring nanoparticles. To solve this problem, one- and two-dimensional superlattice of colloidal nanoparticles were synthesized by using self-assembly methods [12-14] so that desired optoelectronic properties such as proper emission wavelength and large particle size and shape can be achieved. However, three-dimensional self-assembly nanostructures based on PbSe colloidal nanoparticles have rarely been investigated. Self-assembly is currently an efficient method to organize nanoparticles into close-packed and ordered arrays. Generally, the driven forces for self-assembly process include hydrogen-bonding, electrostatic interaction and van der Waals interactions [15-17]. Here, we demonstrated three-dimensional PbSe superlattices in octahedron shape via self-assembly process by using hot solution method. Such self-assembly behavior can be attributed to the interaction between surfactants. In addition, the surface charge may also play an important role in this self-assembly process. Finally, IR photodetector based on this self-assembly superlattices was fabricated with very high detectivity of $4*10^{10}$ Jones at low bias of 3V under 830 nm IR irradiation.

The transmission electron microscope (TEM) images of PbSe superlattices are shown in Fig. 1(a). Each PbSe superlattices consisted of hundreds of PbSe nanoparticles with size of 5 nm, forming clusters with uniform size of 50-60 nm and square shape. Corresponding SEM image was shown in the inset of Fig. 1(a), however, indicating tetrahedron shape of these self-assembly PbSe superlattices. This is inconsistent with the results shown by TEM images. Given these, the best explanation would be the shape of self-assembly superlattices is octahedron, which then exhibits different shapes

*Corresponding Author Lei Qian qian_lei@126.com; Ting Zhang zhangting@bit.edu.cn ; Paul H Holloway pholl@mse.ufl.edu

(tetrahedron or square) from different viewing angles. The high-resolution TEM (HRTEM) image shown in Fig. 1(b) suggests the same orientation of crystal lattice within one colloidal superlattices. This is confirmed by the diffraction pattern of single PbSe superlattices, featuring single-crystal structure, as shown in the inset of Fig. 1(b). It was noticed that the diffraction pattern is slightly broad and arc-like, which implied slight lattice orientation misalignment of PbSe nanoparticles within the self-assembly superlattices. Figure 1(c) showed a single PbSe nanoparticle with good crystallinity with particle size of 5 nm. Lifshitz et al. previously reported spherical shape of self-assembly PbSe superlattices but with random nanoparticle orientation, therefore the Selected Area Electron Diffraction (SAED) pattern showed polycrystalline feature [18]. In contrast, all the PbSe nanoparticles in self-assembly superlattices here show homogeneous crystal orientation, resulting in single crystal feature in the SAED pattern.

X-ray diffraction (XRD) results exhibit that the relative intensity of (111) peak in PbSe self-assembly superlattices increased compared with standard bulk materials, as shown in Fig. 2, suggesting the preferable growth along (111) direction for PbSe superlattices. Therefore, the octahedron structure is formed for PbSe superlattices, instead of the intrinsic cubic structure for bulk PbSe. The size of PbSe crystal domain (not single particle) could be extracted from the XRD results through Scherrer's equation considering each PbSe nanoparticle has the same crystal orientation. The size of each PbSe crystal domain then can be calculated to be ~20 nm. This result is much larger than the one obtained from TEM images but still smaller than the size of self-assembly superlattices. This could attribute to the slight misalignment of PbSe nanoparticles within superlattices.

To further investigate the formation mechanism of such self-assembly PbSe superlattices, we first varied the mixing ratio of surfactants, which have obvious effect on the shape or surface properties of nanomaterials. While keeping the amount of OA for 1.5 mL, the self-assembly PbSe superlattices can only be obtained with TOP to TOPO ratio of 4:4, as shown in Fig 3. Increasing TOP amount will lead to discrete PbSe nanocrystals with different shapes, rather than organized self-assembly cluster. On the other hand, the size of self-assembly superlattices was decreased and finally disappeared with gradually increasing amount of TOPO. Similarly, when the amount of OA was

*Corresponding Author Lei Qian qian_lei@126.com; Ting Zhang zhangting@bit.edu.cn ; Paul H Holloway pholl@mse.ufl.edu

increased from 0.5 mL to 2.5 mL, the size of PbSe self-assembly superlattices were also decreased and no PbSe superlattices could form with 2.5 mL OA, as shown in Fig.4. The interaction between surfactants of adjacent nanoparticles is believed as one of the predominant factors to form self-assembly nanostructure. TOPO has large permanent dipole moment originating from the phosphorus-oxygen (P-O) bond, which might be the primary driven force for the formation of self-assembly superlattices.

Figure 5 shows the TEM images of the temporal evolution of PbSe superlattices formation process. The growth of 5 nm size PbSe nanoparticles are finished within the first 45 seconds and then swiftly self-assembled into uniform shape in the following 45seconds. The size of self-assembly PbSe superlattices gradually increased with reaction time, while there is no more growth for individual PbSe nanoparticle. The evolution of electron diffraction pattern images shows that in the beginning the PbSe nanoparticles were assembled with random crystal orientation, indicated by the feature of continuous circle in ED pattern. Then the pattern of self-assembly superlattices changed to symmetric discrete arcs, which implied that the nanoparticles within the superlattices now have the same crystal orientation.

Furthermore, PbSe superlattices were treated with HCl and NaOH in order to study the effects of their surface charge states. The TEM images are shown in Fig. 6. PbSe superlattices will aggregate with HCl treatment whereas it tends to decompose into individual nanoparticle with NaOH treatment. This can be attributed to surface charges induced by the HCl or NaOH treatment, causing electrostatic forces between nanoparticles. This result demonstrates that the electrostatic interaction is a critical parameter for film self-organization. In addition, this PbSe superlattice is compatible with both polar solvent (ethanol) and non-polar solvent (toluene), as shown in Fig. 7. Generally, the polarity of solvents can affect the formation of self-assembly superlattices. However in the system described here, it didn't act as a predominant factor, since the self-assembly superlattices can be dispersed into both polar and non-polar solvents.

Following the similar method, CdSe and PbTe self-assembly superlattices were also prepared. PbTe self-assembly superlattices with 3-dimensional sphere shape can be achieved while the shape of

*Corresponding Author Lei Qian qian_lei@126.com; Ting Zhang zhangting@bit.edu.cn ; Paul H Holloway pholl@mse.ufl.edu

self-assembly superlattices formed by CdSe nanoparticles only show one-dimensional chain, as shown in Fig. 8. PbTe has the same cubic crystal structure as PbSe while CdSe has hexagonal crystal structure, which might be the reason making such difference.

Figure 9 shows the detectivities as a function of bias for the IR photodetector with device structure ITO/PEDOT:PSS/poly-TPD/PbSe superlattices or PbSe nanoparticles/ZnO nanoparticles/Al under 830 nm IR irradiation. ZnO nanoparticles with size of 2~3 nm are used as electron transport layer in this type of IR photodetector[19-20]. This device exhibits detectivity value of $4*10^{10}$ Jones at -3V for PbSe superlattices, 30% higher than that made by PbSe nanoparticles with 5nm size, which demonstrated that self-assembly nanomaterials not only keep good optical properties of single nanoparticles but also improve charge transport ability, making PbSe superlattices a promising alternative to conventional IR photodetector.

In summary, we synthesized PbSe superlattices with consistent crystal lattice orientation, is driven by interaction between surfactants and surface charges. This method can apply to other IV-VI type semiconductor to achieve 3-D self-assembly superlattices. This novel PbSe superlattices were also used to make IR photodetector, which shows $4*10^{10}$Jones detectivity at -3V under 830 nm IR irradiation.

Experimental Section:

Materials: Lead acetate trihydrate, Selenium, DPE, oleic acid, trioctylphosphine (TOP) and trioctylphosphine oxide (TOPO) were purchased from Aldrich. The solvents including Butanol and Toluene were purchased from Fisher. All the chemicals were used as obtained without any further purification.

Synthesis of three-dimensional PbSe superlattices: In a typical reaction, Lead acetate trihydrate (0.65 g), DPE (2 ml), oleic acid (1.5 ml), TOP (4 ml) and TOPO (4 ml) were added to a three-neck flask and the mixture was heated to 150°C with alternating vacuum and nitrogen flush for half an hour and then kept at 150 °C under vacuum for another one and half hours. Se-TOP precursor solution was made by

*Corresponding Author Lei Qian qian_lei@126.com; Ting Zhang zhangting@bit.edu.cn ; Paul H Holloway pholl@mse.ufl.edu

dissolving Selenium (134.2 mg) in TOP (1.3 ml) and TOPO (0.4 ml) at 150 °C for two hours. Then the Pb and Se precursor solutions were mixed after cooling down to room temperature. 10 mL DPE was added into three-neck flask and heated to 180 °C for one hand half hour and then cool down to 160 °C. The prepared Pb and Se mixture was injected into the reaction flask rapidly, leading the final temperature of reaction mixture down to 120 °C. The aliquots were taken at different reaction time and purified with Butanol and re-dispersed in Toluene without any post-synthesis size-selection procedure.

Sample Characterization: A JEOL 2010F transmission electron microscope operated at 200kV was used for imaging and analysis of the nanoparticles. SEM measurements were performed on a Hitachi S-4000 FE-SEM operated at 6kV. X-ray diffraction (XRD) patterns were obtained with a Philips MRD X'Pert system for information on crystal structure and crystal size. The XRD pattern was collected in the step scan mode, with 2θ scan range of 15-80°, step size of 0.01°, and 1° grazing angle of incident X-rays.

Device fabrication: Photodetector were fabricated on glass substrates commercially pre-coated with a layer of indium tin oxide (ITO) with a sheet resistance of ~20 Ω/sq. The substrates were cleaned with deionized water, acetone, and isopropanol consecutively for 45 min, and then treated in ultraviolet ozone for 15 min before spin-coated by PEDOT:PSS (AI 4803). After baked at 150^{o}C for 15min, the substrates were transferred into glove box for poly-TPD, PbSe superlattices and ZnO NPs layers deposition. Poly-TPD (ADS 254BE) was purchased from ADS and used as obtained. Used as hole-transport layer, poly-TPD (1.5wt% in chlorobenzene) was spin-coated at 2000 rpm for 30 s, followed with annealing process at 110 ^{o}C for 30 min. Then, PbSe superlattices (15mg/ml in Toluene) and ZnO NPs (3 0mg/ml in ethanol) solutions were successively spin-coated with spin speed of 2000 rpm and 4000rpm for 30s, respectively, followed with annealing process at 145 ^{o}C for 30 min. Finally the substrates were loaded into a high vacuum chamber (background pressure ~3×10^{-7} Torr) for the deposition of 100 nm thick aluminum cathode. The Al cathode was deposited through an *in situ*

*Corresponding Author Lei Qian qian_lei@126.com; Ting Zhang zhangting@bit.edu.cn ; Paul H Holloway pholl@mse.ufl.edu

shadow mask, forming an active device area of 4 mm^2.

Device Characterization: All characterization were performed in ambient. The current-voltage (*I–V*) characteristics of the devices were measured with a Keithley 4200 semiconductor parameter analyzer. The devices were irradiated with monochromatic light from single laser source at wavelength of 830 nm with power intensity of 100 μW cm^{-2}. The photocurrent response as a function of bias voltage was measured using a Stanford Research System SR810 DSP lock-in amplifier.

Acknowledgement

This work was financially supported by the research project of the National Natural Science Foundation of China (61376044 and 10904002). T.Z also gratefully acknowledges the Scientific Research Foundation for the Returned Overseas Chinese Scholars of State Education Ministry.

*Corresponding Author Lei Qian qian_lei@126.com; Ting Zhang zhangting@bit.edu.cn ; Paul H Holloway pholl@mse.ufl.edu

References:

[1] L. Bakueva, I. Gorelikov, S. Musikhin, X.S. Zhao, E.H. Kumacheva, *Adv. Mater.* **2004**, 16, 926.

[2] T.C. Harman, P.J. Taylor, M.P. Walsh, B.E. LaForge, *Science* **2002**, 297, 2229.

[3] C.B. Murray, S. Sun, W. Gaschler, H. Doyle, T.A. Betley, C.R. Kagan, *IBM J.Res.Dev.* **2001**, 45, 47.

[4] Y. Wang, A. Tang, K. Li, C. Yang, M. Wang, H. Ye, Y. Hou, F. Teng, *Langmuir* **2012**. 28(47), 16436.

[5] K. Cho, D. Talapin, W. Gaschler, and C. Murray, *J.Am.Chem.Soc.* **2005**, 127(19), 7140.

[6] L. Qian, D. Bera, P.H. Holloway, *Nanotechnology*, **2008**, 19, 285702.

[7] Y. Yin, A.P. Alivisatos, *Nature* **2005**, 437, 664.

[8] W. Lu, J. Fang, Y. Ding, Z. Wang, *J.Phys.Chem.B* **2005**, 109, 19219.

[9] A. Tang, L. Yi, W. Han, F. Teng, Y. Wang, Y. Hou and M. Gao, *Appl.Phys.Lett.* **2010**, 97, 033112.

[10] L. Yi, A. Tang, M. Niu, W. Han, Y. Hou and M. Gao, *CrystEngComm*, **2010**, 12, 4124

[11] A. Tang, S. Qu, K. Li, Y. Hou, F. Teng, J. Cao, Y. Wang and Z. Wang, *Nanotechnology*, **2010**, 21, 285602.

[12] W. lu, P. Gao, W.B. Jian, Z.L. Wang, J. Fang, *J.Am.Chem.Soc.* **2004**, 126, 14816.

[13] E.V. Shevchnko, D.V. Talapin, N.A. Kotov, S. O'Brine, C.B. Murray, *Nature* **2006**, 439, 55.

[14] W. Pusz, A. Kowalewski, P. Martyniuk, W. Gawron, E. Plis, S. Krishna, A. Rogalski, *Opt.Eng.* **2014**, 53(4), 043107.

[15] Z.Y. Tang, Z.L. Zhang, Y. Wang, S.C. Glotzer, N.A. Kotov, *Science* **2006**, 314, 274.

[16] Z.P. Zhang, H.P. Sun, X.Q. Shao, D.F. Li, H.D. Yu, M.Y. Han, *Adv.Mater.* **2005**, 17, 42.

[17] J.Q. Zhuang, H.M. Wu, Y.A. Yang, Y.C. Cao, *J.Am.Soc.Chem.* **2007**, 129, 14166.

[18] A. Sashchiuk, L. Amirav, M. Bashouti, M. Krueger, U. Sivan, E. Lifshitz, *Nano Letters*, **2004**, 4, 159.

[19] L. Qian, Y. Zheng, J. Xue, P.H. Holloway, *Nature Photonics* **2011**, 5(9), 543.

[20] L. Qian, Y. Zheng, K.R. Choudhury, D. Bera, F. So, J. Xue, P.H. Holloway, *Nano Today*, **2010**, 5, 384.

*Corresponding Author Lei Qian qian_lei@126.com; Ting Zhang zhangting@bit.edu.cn ; Paul H Holloway pholl@mse.ufl.edu

Figure Caption:

Fig 1: (a) TEM image of PbSe superlattices (scale bar: 100nm). Inset: SEM image of PbSe superlattices; (b) HRTEM of PbSe superlattices (scale bar: 5 nm). Inset: ED pattern, and (c) HRTEM of single PbSe nanoparticles within superlattices (scale bar: 1 nm).

Fig 2: XRD pattern of PbSe superlattices. Inset: (left) Comparison of XRD peaks between PbSe superlattices and standard bulk PbSe; (right) structure schematics of PbSe superlattices.

Fig 3: TEM images of PbSe nanostructures synthesized with different mixing ratios of TOP to TOPO from 8:0 to 0:8 (Oleic acid was kept at 1.5 ml).

Fig 4: TEM images of PbSe nanostructures synthesized with different amounts of oleic acid from 2.5 ml to 0.5 ml with the TOP:TOPO ratio of 4:4.

Fig 5: TEM images of PbSe superlattices formation evolution: (a) 45s; (b) 90s; (c) 12min; and (d) 24min (Oleic acid = 1.5 ml, TOP:TOPO = 4:4). Inset: corresponding ED patterns.

Fig 6: TEM images of PbSe superlattices treated by (a) HCl and (b) NaOH. HCl could make the surface of nanoparticle more positive charged while NaOH could make it more negative charged.

Fig 7: TEM images of PbSe superlattices dissolved in non-polar solvent: (a) Toluene and

*Corresponding Author Lei Qian qian_lei@126.com; Ting Zhang zhangting@bit.edu.cn ; Paul H Holloway pholl@mse.ufl.edu

polar solvent: (b) Toluene/ethanol. Polarity of solvents might provide the driven force for the formation of self-assembly nanostructure to some extent but it did not play the same role in our PbSe superlattices system.

Fig 8: TEM images of (a) PbTe and (b) CdSe nanomaterials synthesized by the same method.

Fig 9: Detectivity of PbSe superlattices/nanoparticles based IR photodetector as a function of bias under 830 nm IR irradiation. Red open circle: PbSe superlattices; black solid square: PbSe nanoparticles.

*Corresponding Author Lei Qian qian_lei@126.com; Ting Zhang zhangting@bit.edu.cn ; Paul H Holloway pholl@mse.ufl.edu

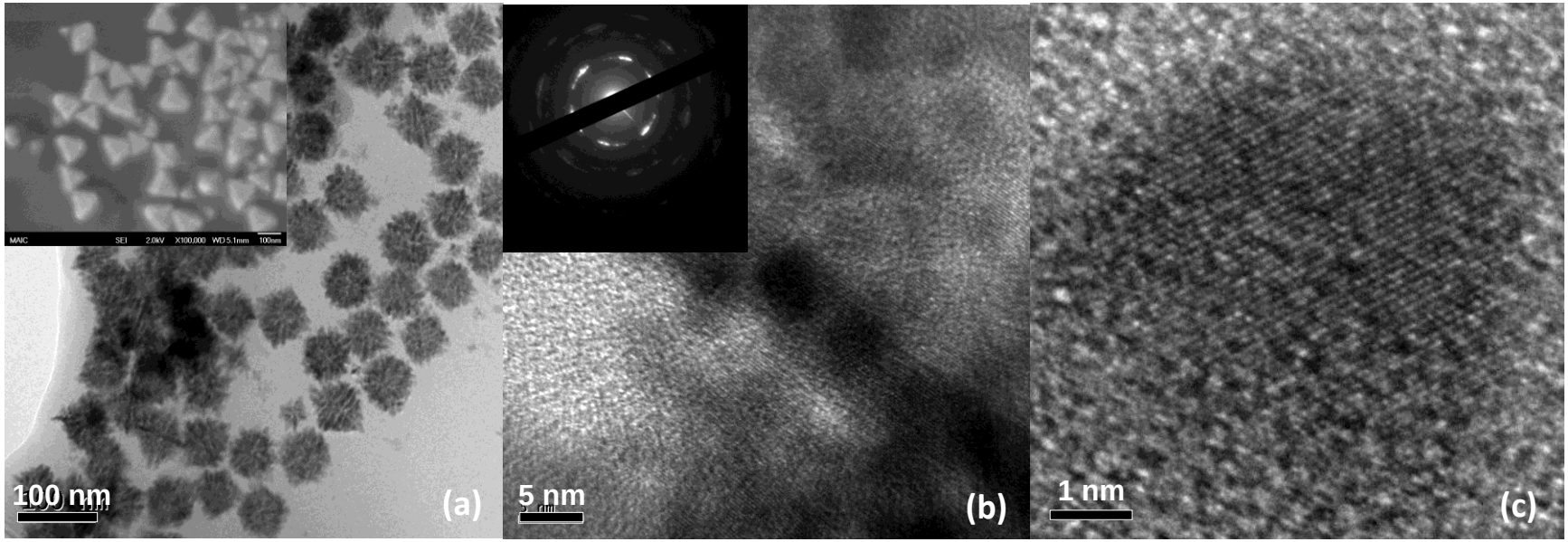

Qian et al., Figure 1

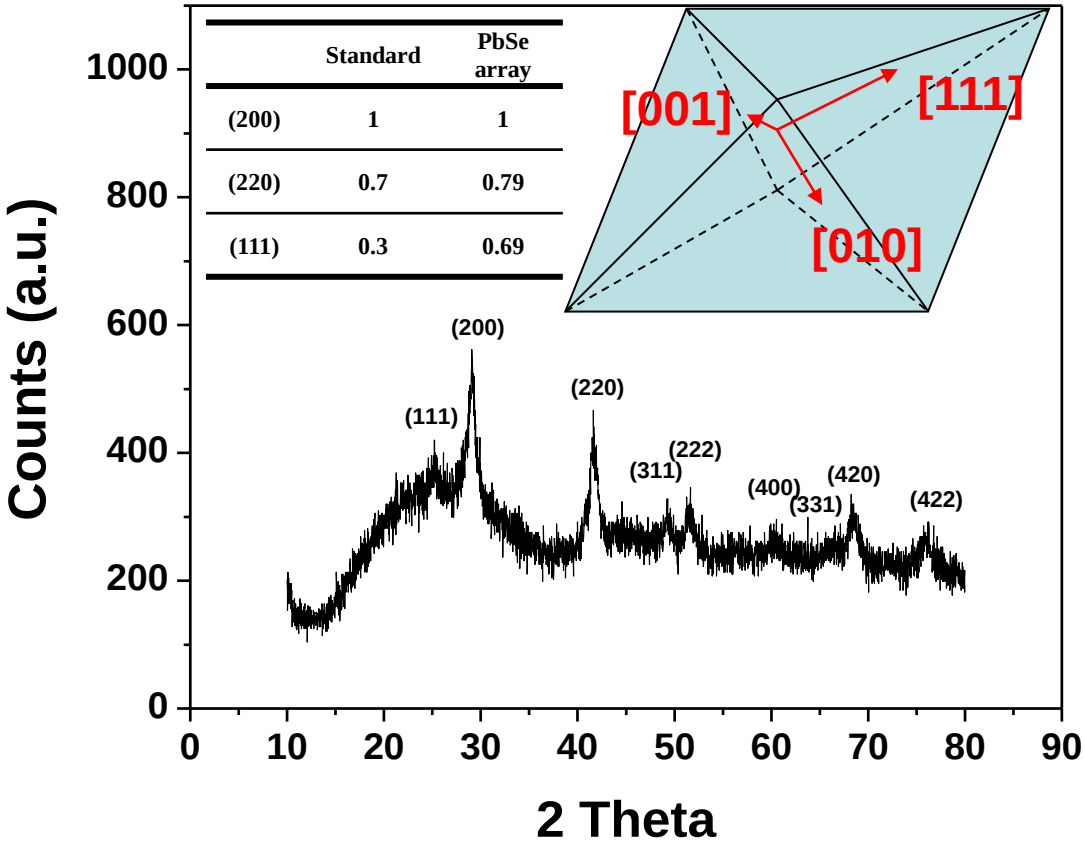

Qian et al., Figure 2

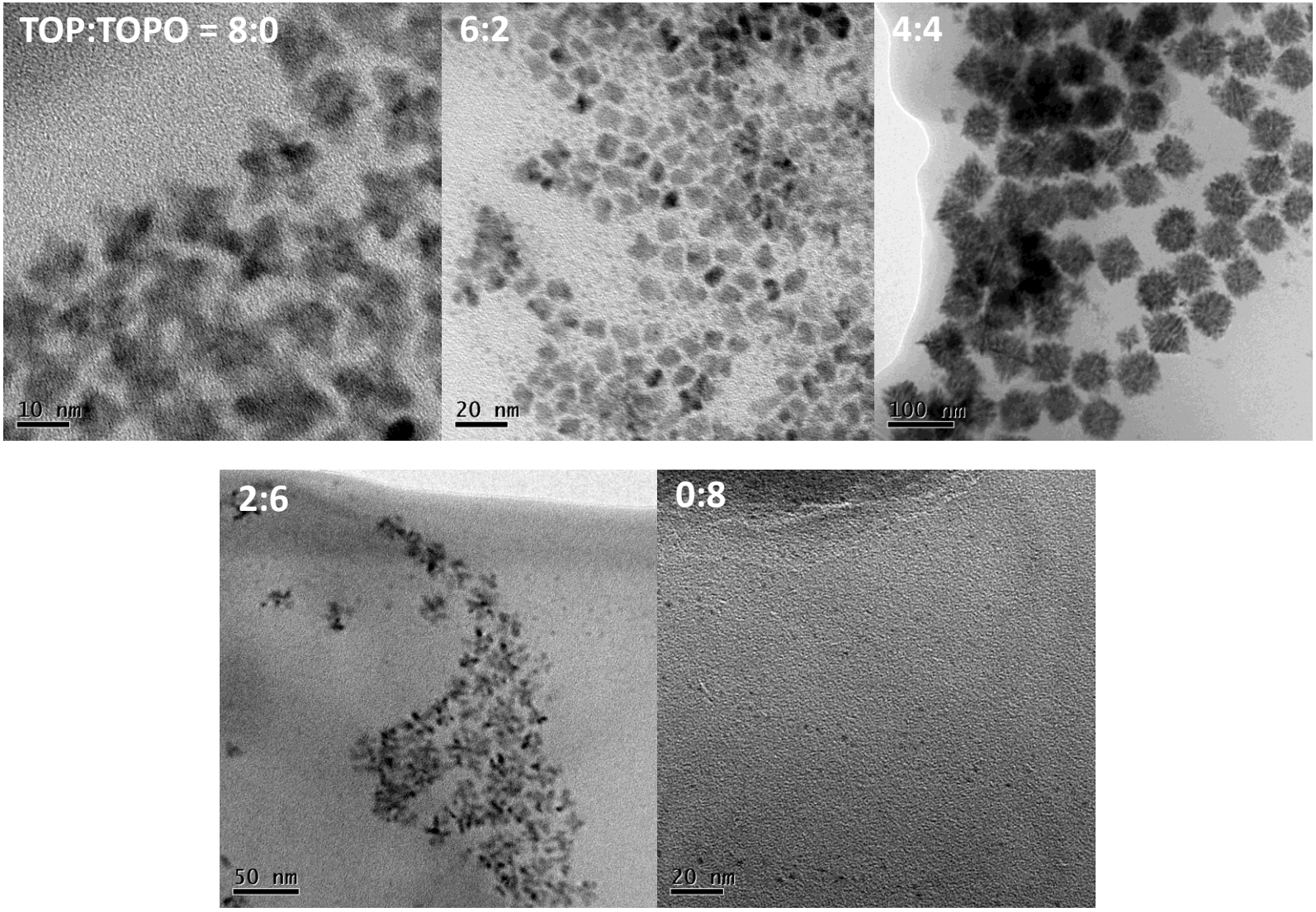

Qian et al., Figure 3

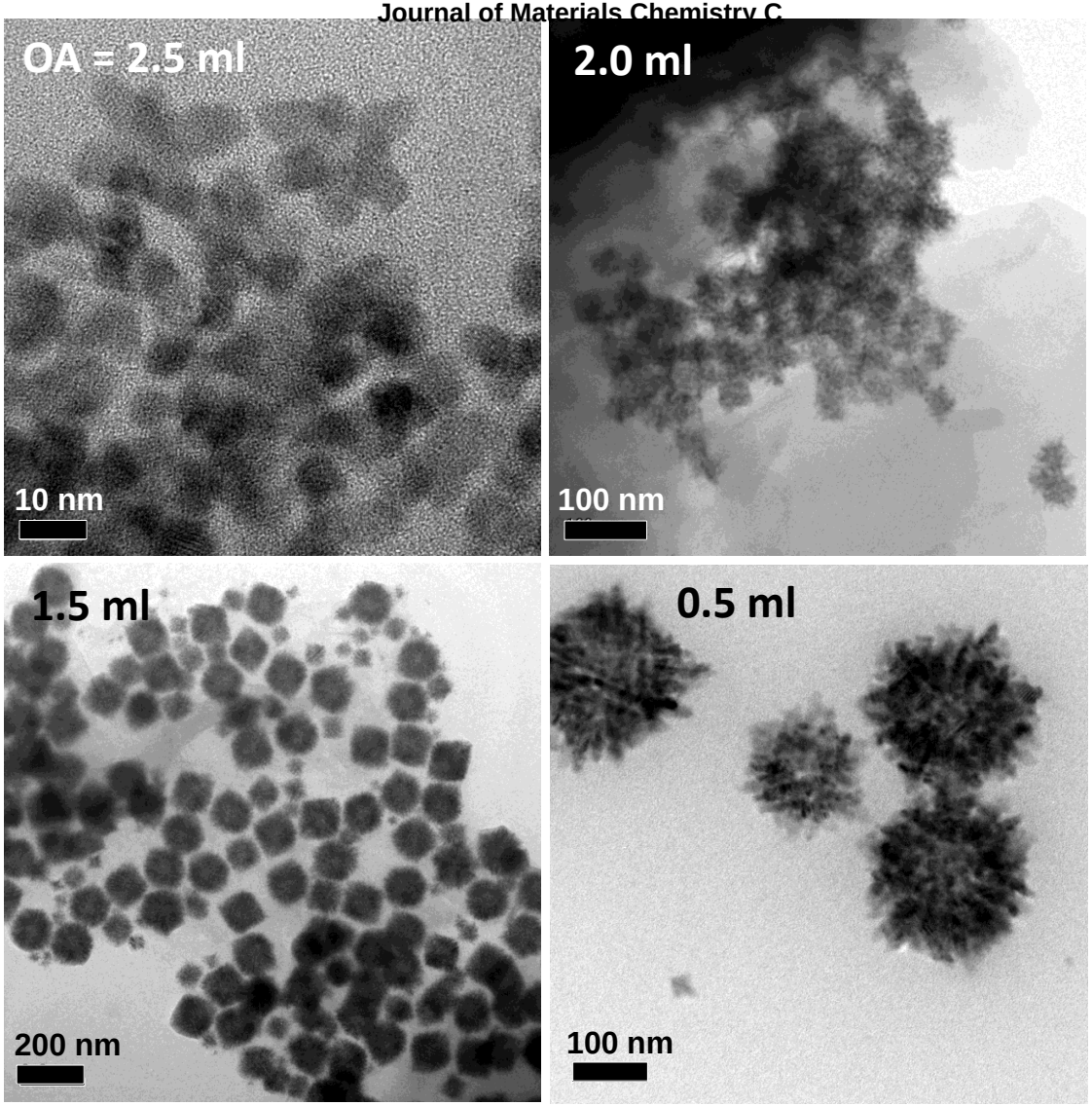

Qian et al., Figure 4

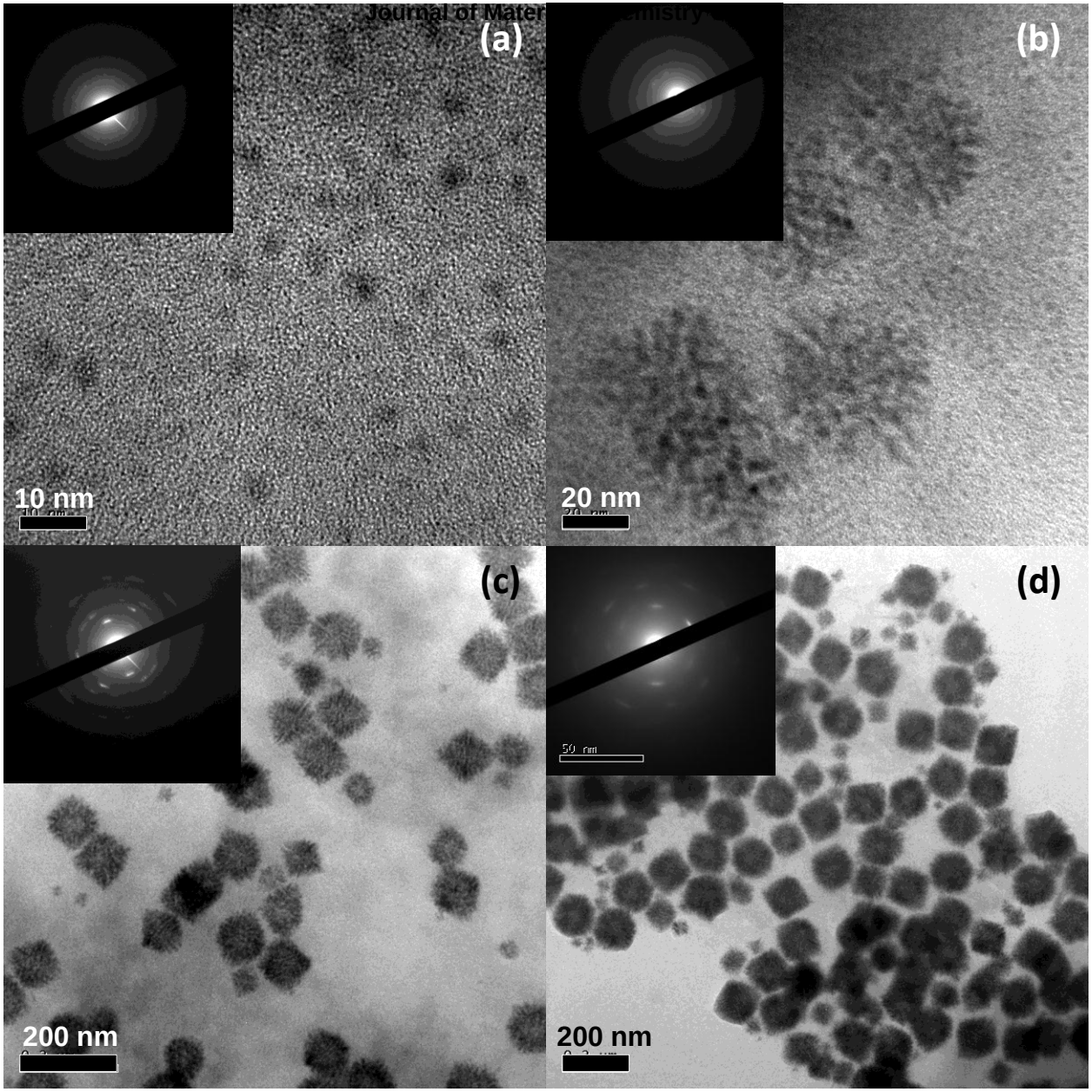

Qian et al., Figure 5

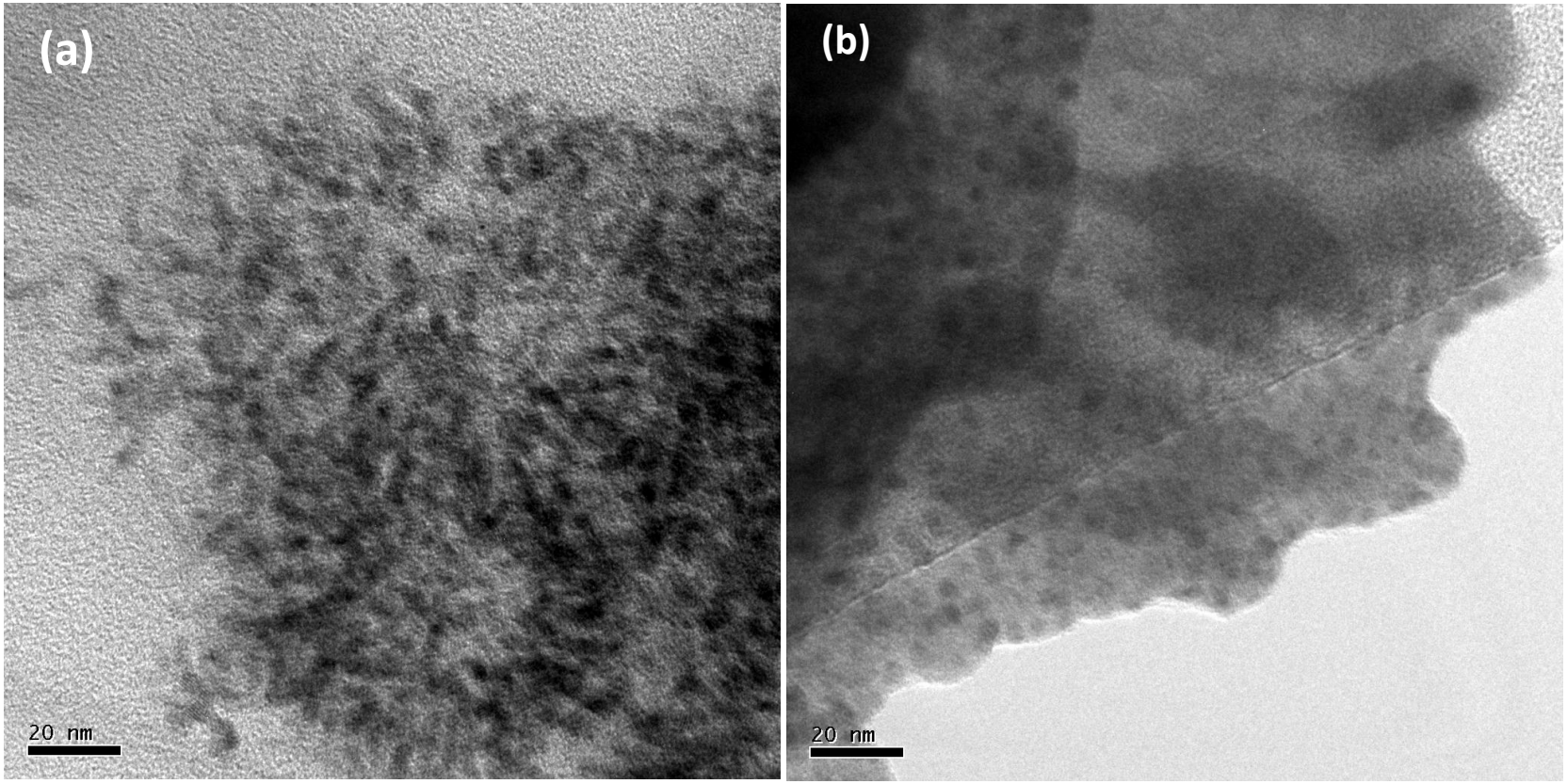

Qian et al., Figure 6

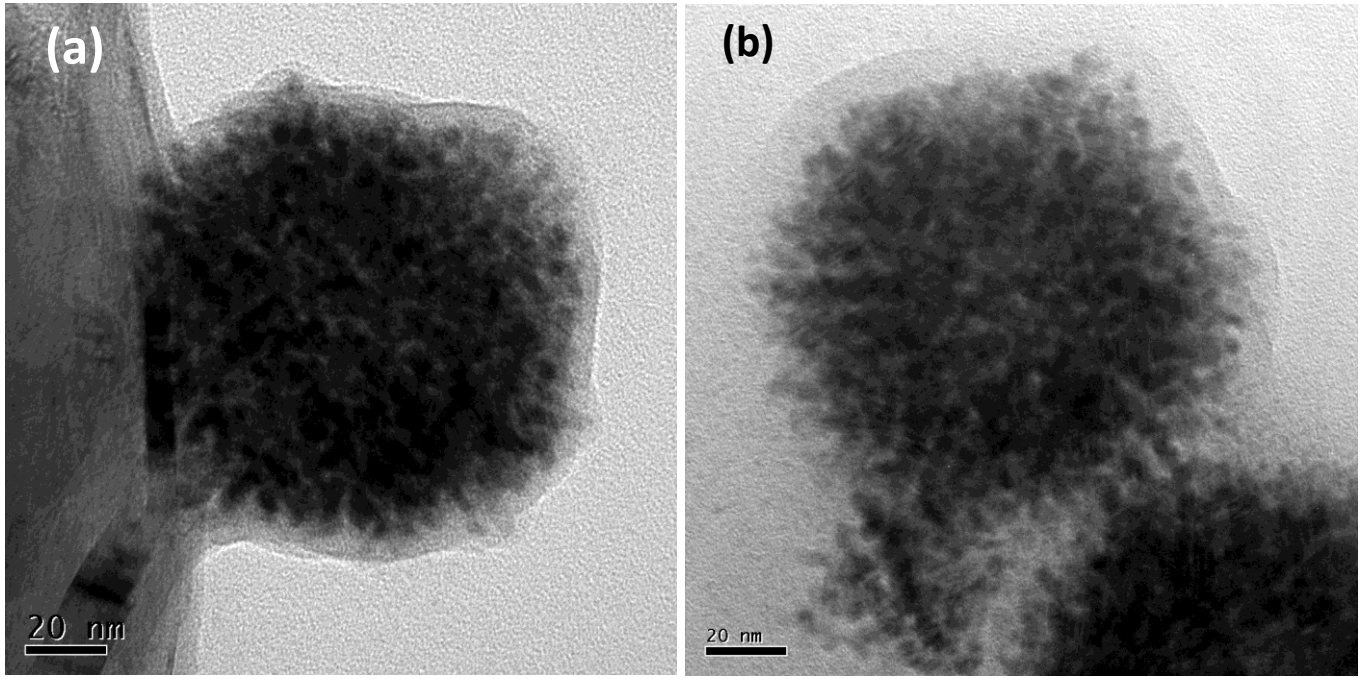

Qian et al., Figure 7

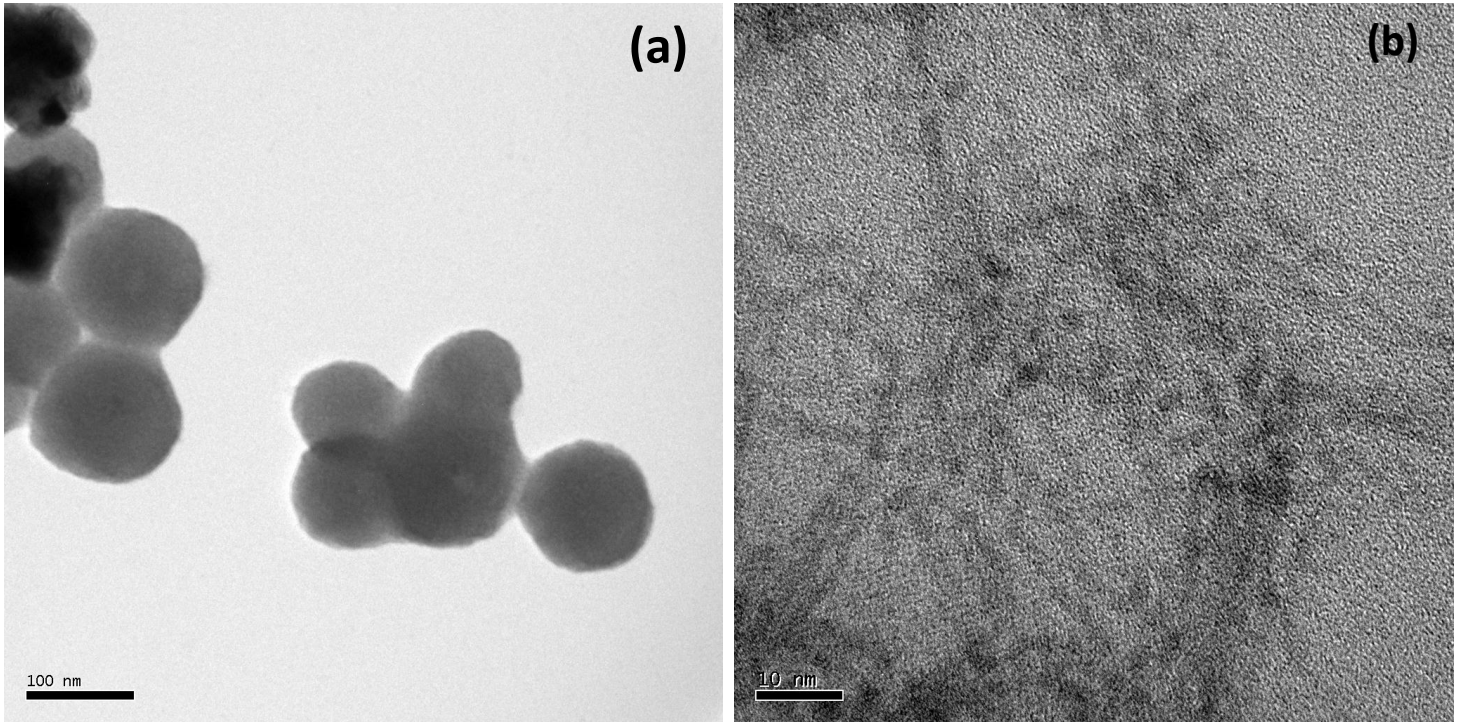

Qian et al., Figure 8

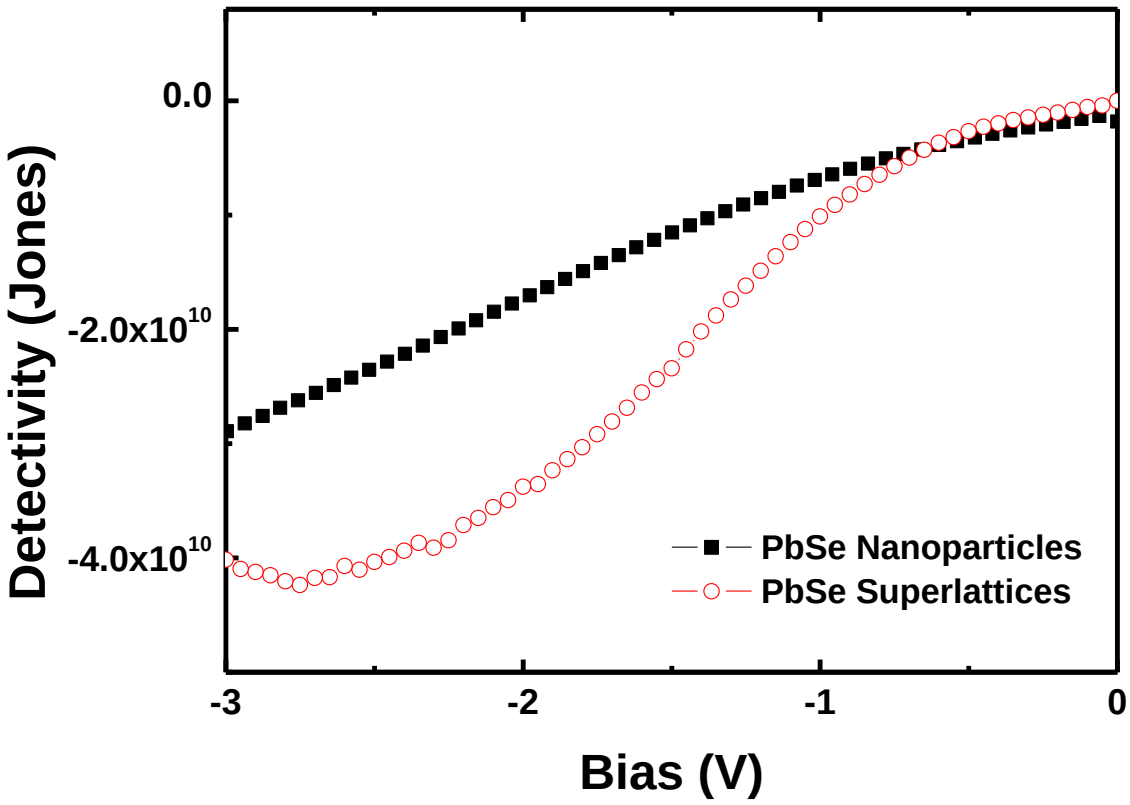

Qian et al., Figure 9

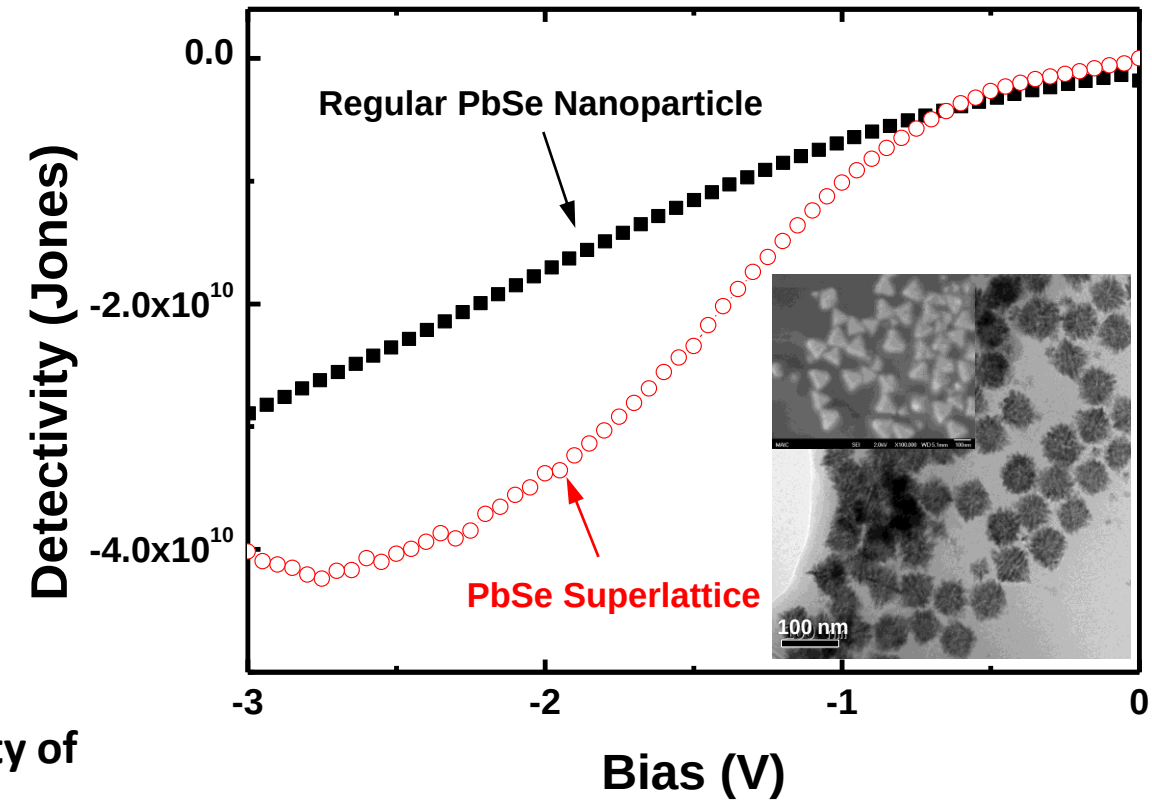

- **Highly improved detectivity of Infrared photodetector by using three-dimensional self-assembly PbSe superlattices.**